

## Rechargeable Batteries Driven by Redox Reactions of Mn<sub>12</sub> Clusters with Structural Changes: XAFS Analyses of the Charging/Discharging Processes in Molecular Cluster Batteries

Hirofumi Yoshikawa,<sup>\*,†</sup> Shun Hamanaka,<sup>†</sup> Yasuhito Miyoshi,<sup>†</sup> Yoshihiko Kondo,<sup>†</sup> Satoru Shigematsu,<sup>‡</sup> Nao Akutagawa,<sup>‡</sup> Masaharu Sato,<sup>‡</sup> Toshihiko Yokoyama,<sup>§</sup> and Kunio Awaga<sup>\*,†</sup>

<sup>†</sup>Department of Chemistry & Research Center for Materials Science, Graduate School of Science, Furo-cho, Chikusa-ku, Nagoya 464-8602, Japan, <sup>‡</sup>Section I Office of Energy Device Development, Research & Development Center, Murata Manufacturing Company, Ltd., Yasu 2288, Oshinohara, Yasu-shi, Shiga 520-2393, Japan, and <sup>§</sup>Institute for Molecular Sciences, Okazaki 444-8585, Japan

Received July 4, 2009

Molecular clusters such as the Mn<sub>12</sub> cluster (Mn<sub>12</sub>) can be used as a cathode-active material in Li batteries. X-ray absorption fine structure studies on the cathode materials in Mn<sub>12</sub> molecular cluster batteries demonstrated that the charging/discharging processes include four-electron-redox reaction of Mn<sub>12</sub> with a significant change in its molecular structure.

Recently, much attention has been focused on the creation of new energy systems, such as high-performance rechargeable batteries, as a solution to the global energy and environmental crises.<sup>1</sup> Li ion batteries are already widely used because of their good cyclability and high voltage.<sup>2,3</sup> However, while this rechargeable battery can provide high capacity, its charging/discharging rate is slow because the charging/discharging process includes absorption/desorption of Li ions into/from the cathode-active material, LiCoO<sub>2</sub>. In addition, Co is toxic and expensive; therefore, much effort has been devoted to the development of low-cost, environmentally friendly cathode materials that can realize both quick charging/discharging and high power density.<sup>1</sup>

Redox-active molecular materials are good candidates for a high-performance cathode-active material. Recently, organic radical batteries have been developed as a new type of rechargeable Li battery, in which organic polymers carrying stable nitroxyl radicals are utilized as a cathode-active material.<sup>4–6</sup>

Because of the smooth and fast electrochemical reactions of the organic radicals, the new batteries are quickly chargeable/dischargeable. However, their capacities (<100 Ah/kg) are lower than those of the Li ion batteries (180 Ah/kg) probably because the rather large radical moiety (molecular weight = ca. 200) can store only one or two electrons in the redox reaction.

To achieve both high capacity and fast charging/discharging, we have previously proposed the use of polynuclear metal complex clusters (molecular clusters that are small aggregates of metal ions connected by organic ligands) that undergo multistep redox reactions as a cathode-active material for Li batteries. In our previous paper,<sup>7</sup> we reported the fabrication of a molecular cluster battery (MCB) in which the cathode-active material is [Mn<sub>12</sub>O<sub>12</sub>(CH<sub>3</sub>COO)<sub>16</sub>(H<sub>2</sub>O)<sub>4</sub>] (abbreviated as Mn<sub>12</sub>Ac). This molecule is a well-known single-molecule magnet<sup>8</sup> and exhibits a multistep redox reaction.<sup>9</sup> The MCBs of Mn<sub>12</sub>Ac were found to show an extremely high capacity of ca. 200 Ah/kg in the first discharge, which is higher than that of the usual Li ion batteries, though the capacities of the second run and after were ca. 70 Ah/kg.

In the present work, we carried out ex situ X-ray absorption fine structure (XAFS) analyses of the charging/discharging processes of the Mn<sub>12</sub> MCBs to reveal the microscopic mechanisms of their battery performance. XAFS analysis is an appropriate technique for observing valence changes and local structures of nanoscale or highly disordered compounds such as battery-active materials.<sup>10</sup> Two different regions of the K-edge absorption spectra of Mn are useful: X-ray

\*To whom correspondence should be addressed. E-mail: yoshikawah@mbox.chem.nagoya-u.ac.jp (H.Y.), awaga@mbox.chem.nagoya-u.ac.jp (K.A.).

(1) Tarascon, J.-M.; Armand, M. *Nature (London)* **2001**, *414*, 359.  
(2) Manthiram, A. *NATO Sci. Ser. II* **2002**, *61*, 157.  
(3) Brodd, R. J.; Tagawa, K. In *Advances in Lithium-Ion Batteries*; van Schalkwijk, W., Scrosati, B., Eds.; Kluwer Academic/Plenum Publishers: New York, 2002; p 267.  
(4) Nishide, H.; Iwasa, S.; Pu, Y.-J.; Suga, T.; Nakahara, K.; Satoh, M. *Electrochim. Acta* **2004**, *50*, 827.  
(5) Nakahara, K.; Iwasa, S.; Satoh, M.; Morioka, Y.; Iriyama, J.; Suguro, M.; Hasegawa, E. *Chem. Phys. Lett.* **2002**, *359*, 351.  
(6) Katsumata, T.; Satoh, M.; Wada, J.; Shiotsuki, M.; Sanda, F.; Masuda, T. *Macromol. Rapid Commun.* **2006**, *27*, 1206.

(7) Yoshikawa, H.; Kazama, C.; Awaga, K.; Satoh, M.; Wada, J. *Chem. Commun.* **2007**, 3169.  
(8) Caneschi, A.; Gatteschi, D.; Sessoli, R.; Barra, A. L.; Bruel, L. C.; Guillot, M. *J. Am. Chem. Soc.* **1991**, *113*, 5873.  
(9) Sessoli, R.; Tsai, H.-L.; Schake, A. R.; Wang, S.; Vincent, J. B.; Folting, K.; Gatteschi, D.; Christou, G.; Hendrickson, D. N. *J. Am. Chem. Soc.* **1993**, *115*, 1804.  
(10) Islam, M. S.; Ammundsen, B.; Jones, D. J.; Roziere, J. In *Materials for Lithium-Ion Batteries*; Julien, C.; Stoyanov, Z., Eds.; Kluwer Academic Publishers: Amsterdam, The Netherlands, 2000; p 279.

absorption near-edge structure (XANES) and extended X-ray absorption fine structure (EXAFS). On the basis of the results of our analysis, we discuss the oxidation states of the Mn ions and the bond lengths in Mn12 in the electrochemical charging/discharging process of Mn12 MCBs.

Mn12Pe<sup>t</sup> ([Mn<sub>12</sub>O<sub>12</sub>(CH<sub>3</sub>CH<sub>2</sub>C(CH<sub>3</sub>)<sub>2</sub>COO)<sub>16</sub>(H<sub>2</sub>O)<sub>4</sub>) with a bulky *tert*-pentyl carboxylate ligand was used as a cathode-active material for XAFS studies because it was found to be more stable than Mn12Ac. Figure 1a shows the charge/discharge curves for a Mn12Pe<sup>t</sup>/Li battery at a constant current of 0.1 mA in the voltage range of 2.0–4.2 V. The black curve shows the charge for the as-prepared cell; the voltage quickly exceeds 4.2 V from the initial high voltage (3.5 V). It is likely that this battery was already charged in the fabrication process of the coin cell. The red curve shows the first discharging process; the voltage exhibits a gradual decrease, making a narrow plateau at ca. 3.2 V, indicating a large capacity of ca. 150 Ah/kg. The blue and pink curves in Figure 1a indicate the second charging and discharging processes, respectively. In charging, the voltage exhibits a quick increase to ca. 3.4 V, followed by a gradual increase, and, in discharging, the voltage decreases gradually, indicating a capacity of ca. 110 Ah/kg. This value is much lower than that for the first discharging but is still comparable to those of organic radical batteries.<sup>4–6</sup> The cycle performance for the charging/discharging processes is shown in Figure S1 in the Supporting Information. After the significant decrease at the second cycle, the capacity exhibits a much more gradual decrease. These charging/discharging curves and cycle performances are nearly the same as those of the previous Mn12Ac battery.<sup>7</sup>

To probe the electronic and structural changes of Mn12Pe<sup>t</sup> in the charging/discharging process, we performed XAFS measurements on the cathode material after the first charging (1C)/discharging (1D) and after the second charging (2C)/discharging (2D). These samples were prepared separately; after the charging/discharging operation, each sample was taken from the coin cell and was subjected to the ex situ XAFS measurements. Figure 1b shows the Mn K-edge XANES spectra of 1C, 1D, 2C, 2D, and as-prepared Mn12Pe<sup>t</sup>. The spectrum of 1C is similar to that of Mn12Pe<sup>t</sup>, but after the first discharging, the spectrum of 1D is significantly different from that of 1C. The spectra of 2C and 2D are nearly the same as those of 1C and 1D, respectively.

It is known that the absorption edge energy of the XANES spectra decreases with a decrease in the Mn oxidation state.<sup>11</sup> Figure S2 in the Supporting Information shows the linear relation between the Mn valence and the edge energy, which was obtained in the measurements for the reference materials MnO, Mn<sub>3</sub>O<sub>4</sub>, Mn<sub>2</sub>O<sub>3</sub>, and MnO<sub>2</sub>. From the absorption edges of Mn12Pe<sup>t</sup>, 1C, 1D, 2C, and 2D, which are defined as the point of the largest gradient of the absorption curve, their average Mn valences are calculated, as shown in Figure 1c. There is no significant valence change between Mn12Pe<sup>t</sup> and 1C, which is in agreement with the small voltage change in the first charging. It is considered that Mn12Pe<sup>t</sup> in the as-prepared battery is in the neutral state. The average valence shows a decrease of 0.34 after the first discharging (1D) and returns to the original value after the second charging (2C). A good repeatability is observed in the change from 2C to 2D. The valence change of 0.34 per Mn atom indicates that one

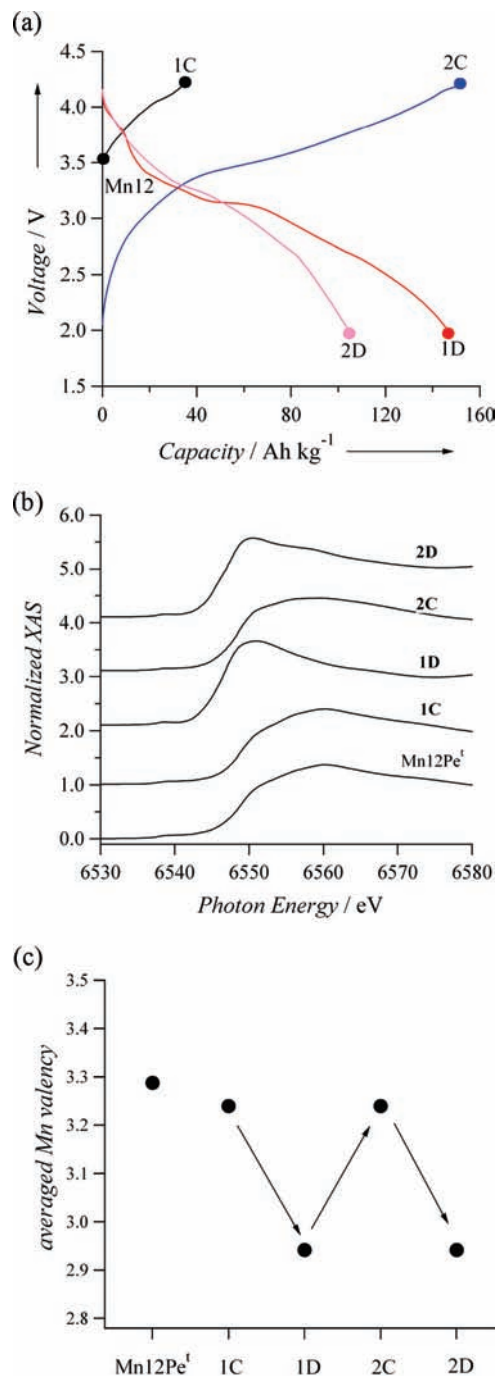


**Figure 1.** (a) Charging/discharging curves of a Mn12Pe<sup>t</sup>/Li MCB. (b) Normalized Mn K-edge XANES spectra for Mn12Pe<sup>t</sup> and the cathode materials after the first charging (1C), the first discharging (1D), the second charging (2C), and the second discharging (2D). (c) Averaged Mn valences of Mn12Pe<sup>t</sup>, 1C, 1D, 2C, and 2D.

Mn12Pe<sup>t</sup> molecule exhibits a valence change of ca. 4 in the discharging/charging processes.<sup>12</sup> On the basis of this value, the theoretical value of the battery capacity is predicted to be ca. 40 Ah/kg, which is much smaller than the large capacities shown by 1D and 2D. A possible reason for the excess capacity is the formation of electrical double layers at the interface between microcrystals of Mn12. Another possible reason is a parasitic charge due to electrochemical side reactions.<sup>13</sup>

(11) Belli, M.; Scafati, A.; Bianconi, A.; Mobilio, S.; Palladino, L.; Reale, A.; Burattini, E. *Solid State Commun.* **1980**, *35*, 355.

(12) Bagai, R.; Christou, G. *Inorg. Chem.* **2007**, *46*, 10810–10818.

(13) Braun, A.; ShROUT, S.; Fowlks, A. C.; Osaisai, B. A.; Seifert, S.; Granlund, E.; Cairns, E. J. *J. Synchrotron Radiat.* **2003**, *10*, 320.

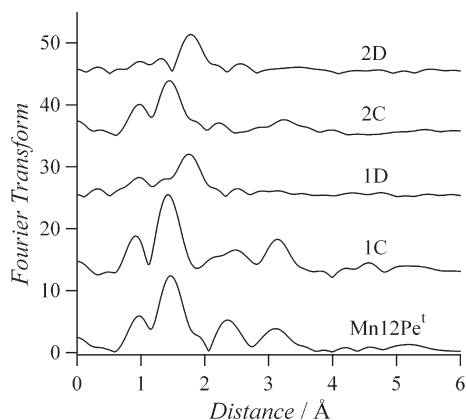


**Figure 2.** Fourier transforms of the Mn K-edge EXAFS spectra for Mn12Pe<sup>I</sup>, 1C, 1D, 2C, and 2D.

It is characteristic of Mn12 MCBs that the redox of the organic part would be incorporated in the battery performance.

EXAFS analyses were performed in order to reveal structural changes in the Mn12Pe<sup>I</sup> molecule. EXAFS functions of  $k^3\chi(k)$  (where  $k$  is the photoelectron wavenumber) were obtained by the standard procedures of pre-edge baseline subtraction, edge-energy determination, post-edge background subtraction (cubic spline), and normalization using the atomic absorption coefficients. Figure S3 in the Supporting Information depicts the  $k^3\chi(k)$  functions for the experimentally obtained Mn absorptions. Fourier transforms of the  $k^3\chi(k)$  functions (the  $k$  range is around 2.5–11.0 Å<sup>-1</sup>) are given in Figure 2. Mn12Pe<sup>I</sup> exhibits four main peaks at 1.0, 1.5, 2.4, and 3.1 Å. The two peaks at 1.0 and 1.5 Å are assignable to the Mn–O distances, while the other two shells at 2.4 and 3.1 Å are assignable to those of Mn–Mn. The curve shapes and peak positions for 1C are similar to those for Mn12Pe<sup>I</sup>, although a shoulder peak appears around 2.4 Å. After the first discharging process, 1D exhibits a completely different curve; the four major peaks of 1C nearly disappear, and a new peak comes out at 1.8 Å, which is assignable to an Mn–O distance. Although we obtained EXAFS spectra of

the well-known one-electron-reduced Mn12 cluster, Mn12Ph<sup>-</sup> ([Mn<sub>12</sub>O<sub>12</sub>(C<sub>6</sub>H<sub>5</sub>COO)<sub>16</sub>(H<sub>2</sub>O)<sub>4</sub>]<sup>-</sup>),<sup>14</sup> structural features in 1D were significantly different from those in the reduced one, as shown in Figure S4 in the Supporting Information. It suggests a drastic transformation of the molecular structure after discharging. After the second charging, the Mn–O and Mn–Mn peaks recover in 2C, although the peak intensities are slightly weakened compared with those of 1C. This indicates a recovery of the molecular structure of Mn12 after charging.

It is worth comparing the redox processes in the Mn12 battery with those of LiMn<sub>2</sub>O<sub>4</sub>, which is a cathode of Li ion batteries. It is known that the Mn valence varies between 3.5 and 4.0 in LiMn<sub>2</sub>O<sub>4</sub>,<sup>15</sup> while Mn12 MCBs operate between 2.9 and 3.3 (Figure 1c). It is also known that the EXAFS spectra of LiMn<sub>2</sub>O<sub>4</sub> include a strong peak at 2.5 Å, which is ascribed to a Mn–Mn distance.<sup>15,16</sup> This feature is also very different from that in the EXAFS spectrum of the Mn12 battery (Figure 2).

In summary, XAFS studies on the rechargeable Mn12Pe<sup>I</sup> battery revealed repeatable redox changes of the Mn12 molecule in the charging/discharging processes. This MCB is concluded to be driven by approximately four-electron redox of Mn12Pe<sup>I</sup>, while the large capacity in the first discharging cannot be explained by this value. The EXAFS spectra suggest a significant structural change of Mn12Pe<sup>I</sup>, which is, however, repeatable in the redox process.

**Acknowledgment.** This work has been performed with the approval of PF PAC (Proposal No. 2008G586). The authors are grateful to the Ministry of Education, Culture, Sports, Science and Technology (MEXT) of Japan for a Grant-in-Aid for Scientific Research.

**Supporting Information Available:** Battery and XAFS analysis methods, theoretical capacity calculations, and Figures S1–S4. This material is available free of charge via the Internet at <http://pubs.acs.org>.

(15) Shiraishi, Y.; Nakai, I.; Tsubata, T.; Himeda, T.; Nishikawa, F. *J. Solid State Chem.* **1997**, *133*, 587–590.

(16) Shiraishi, Y.; Nakai, I.; Tsubata, T.; Himeda, T.; Nishikawa, F. *J. Power Sources* **1999**, *81–82*, 571–574.

(14) Eppley, H. J.; Tsai, H.-L.; de Vries, N.; Folting, K.; Christou, G.; Hendrickson, D. N. *J. Am. Chem. Soc.* **1995**, *117*, 301.